Cathode Materials

DOI: 10.1002/anie.201205292

Confining Sulfur in Double-Shelled Hollow Carbon Spheres for Lithium–Sulfur Batteries**

Chaofeng Zhang, Hao Bin Wu, Changzhou Yuan, Zaiping Guo, and Xiong Wen (David) Lou**

Lithium–sulfur (Li–S) batteries are considered to be a promising energy-storage solution for the rapidly growing demand for energy, which utilize elemental sulfur as the active cathode material to reversibly react with lithium.[1–3] Assuming sulfur can maximally interact with two lithium atoms per sulfur atom, the reversible electrochemical reaction, denoted as $S_8 + 16\,Li \leftrightarrow 8\,Li_2S$, can deliver an exceptionally high capacity of 1672 mA h g^{-1} at around 2.2 V versus Li/Li^+.[4–6] Additionally, the wide-spread availability, low price, and nontoxicity of elemental sulfur make it attractive for large-scale practical applications.

However, the poor electronic/ionic conductivity of elemental sulfur severely limits the practical use of sulfur in an electrode.[7] Another problem of Li–S batteries is the high solubility of long-chain polysulfides (Li_2S_n, $3 \le n \le 6$), which are intermediates of the electrochemical reactions, in conventional organic electrolytes.[3] The dissolved polysulfide ions shuttle between the sulfur cathode and lithium anode, thus causing precipitation of insoluble and insulating Li_2S_2/Li_2S on the surface of the electrodes.[8] This undesirable phenomenon not only results in low Coulombic efficiency and loss of active material, but also hampers the ionic accessibility of the electrodes.[9] Consequently, low specific capacity and fast capacity fading are commonly found in sulfur cathodes.[5,9] Recently, significant advances have been achieved using porous carbon materials as hosts for sulfur, to partly overcome the above-mentioned drawbacks in Li–S batteries.[6,10,11] These carbon hosts are commonly believed to play dual roles in the sulfur–carbon composites: the porous structure of the carbon hosts effectively contains sulfur, the active material, and suppresses the diffusion of polysulfides; meanwhile the carbon framework greatly facilitates electron transport, thus promoting the redox processes in the electrode.[6] As a result, the effective use of sulfur and the cycling stability are substantially improved.

Recent results suggest that the characteristics of the carbon hosts, such as the dimension, morphology, porosity, and texture, are critically important to the electrochemical performance of sulfur–carbon composite electrodes.[11–19] For example, by containing sulfur in porous hollow carbon spheres the sulfur–carbon nanocomposite shows outstanding cycling performance and rate capability.[11] Other carbon materials with hollow structures, such as disordered carbon nanotubes and hollow carbon nanofibers,[14,17] have been investigated as promising carbon hosts for sulfur. These encouraging results suggest the benefits of hollow carbon structures, which might have several advantages including superior confinement ability, a large contact area with the sulfur, and a short transport length for Li^+ ions.

Herein, we report the rational design and synthesis of a new sulfur–carbon nanocomposite by confining sulfur in double-shelled hollow carbon spheres (DHCSs). Such hollow carbon spheres with complex shell structures could maximize the advantages of hollow nanostructures.[20–22] Specifically, the flexible double shells could effectively encapsulate a relatively high amount of sulfur, suppress the outward diffusion of polysulfides, and withstand volume variation upon prolonged cycling. When evaluated as a cathode material for Li–S batteries, this nanocomposite shows significantly improved electrochemical performance.

The double-shelled hollow carbon spheres are prepared using SnO_2 hollow spheres as the hard templates.[23–25] First, SnO_2 hollow spheres with sizes ranging from 300 to 500 nm were synthesized using a facile one-pot template-free approach we developed previously (see Supporting Information, Figure S1 A).[23,25] The porous SnO_2 hollow spheres are then uniformly coated with a glucose-derived polysaccharide on both the interior and exterior surfaces, as well as in the pores within the SnO_2 shell (Figure S1 B).[24] An annealing process in H_2/N_2 gas results in the carbonization of the polysaccharide component and the reduction of SnO_2 into metallic Sn.[26] The Sn particles can be easily dissolved in hydrochloric acid to generate double-shelled hollow carbon spheres (DHCSs), which perfectly replicate the morphology and size of the SnO_2 hollow spheres (Figure S1 C). These unique hollow spheres with two well-defined concentric shells with a distance between them of ca. 50–100 nm could be clearly seen from the transmission electron microscope (TEM) image (Figure 1 A). Both the outer and inner shells showed low contrast under the TEM observation, suggesting that the shells are thin and probably a soft and flexible texture. The contrast within the inter-shell cavity indicated the presence of carbon "links" connecting the two shells.

[*] C. F. Zhang,[+] Prof. Z. P. Guo
Institute for Superconducting & Electronic Materials,
University of Wollongong
Wollongong, NSW 2522 (Australia)
E-mail: zguo@uow.edu.au
C. F. Zhang,[+] H. B. Wu,[+] Dr. C. Z. Yuan, Prof. X. W. Lou
School of Chemical and Biomedical Engineering,
Nanyang Technological University
70 Nanyang Drive, Singapore 637457 (Singapore)
E-mail: xwlou@ntu.edu.sg
Homepage: http://www.ntu.edu.sg/home/xwlou
[+] These authors contributed equally to this work.

[**] Z.P.G. acknowledges financial support from the Australian Research Council through a Discovery Project (DP1094261).

Supporting information for this article (experimental details) is available on the WWW under http://dx.doi.org/10.1002/anie.201205292.

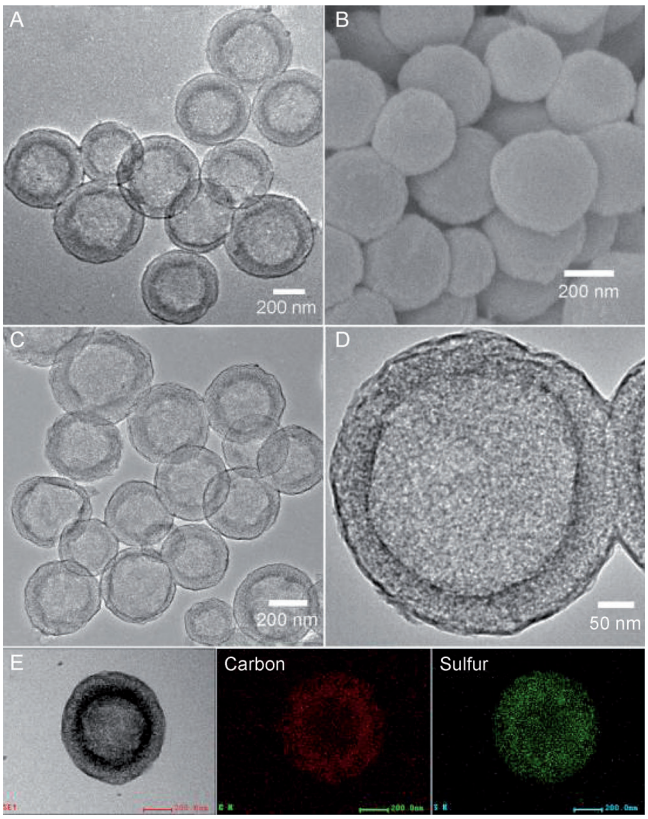

Figure 1. A) TEM image of DHCSs. B) FESEM and C,D) TEM images of the DHCS-S composite. E) TEM image and corresponding elemental mapping of a single DHCS-S sphere.

Thus, a highly porous framework was formed within the two concentric shells, providing an excellent carbon matrix for sulfur loading. The DHCS sample showed a very high Brunauer–Emmett–Teller (BET) specific surface area of 748 $m^2 g^{-1}$ and a large total pore volume of 1.685 $cm^3 g^{-1}$ (a nitrogen adsorption–desorption isotherm is given in Figure S2), again suggesting the excellent potential for sulfur encapsulation.

Sulfur impregnation of the DHCSs was performed at 400 °C, to facilitate the infusion of sulfur into the carbon structure and achieve better encapsulation of sulfur.[14] After the high-temperature sulfur impregnation, the nanocomposite material, denoted as DHCS-S, was characterized in detail. Both field-emission scanning electron microscope (FESEM) and TEM images (Figure 1 B,C) showed similar morphology and structure compared to the pristine DHCS sample. In the magnified TEM image (Figure 1 D), the double-shelled structure can still be easily recognized. No discernible sulfur particles were found inside or outside the hollow spheres, which suggested the uniform dispersion of sulfur onto the carbon matrix. Elemental mapping clearly revealed the presence and uniform distribution of sulfur over a large area (Figure S3). The detailed spatial distribution of sulfur in the DHCSs was further shown by elemental mapping on a single DHCS-S sphere. As depicted in Figure 1 E, both the carbon and sulfur were mainly distributed in the region between the two carbon shells, while the weaker signal in the center suggests that the inner cavity remains hollow. Moreover, the similar distribution of these two elements indicated the high affinity of sulfur for carbon, and the sulfur was well confined in the porous carbon matrix formed by the double-shelled structure.

The powder X-ray diffraction (XRD) patterns of the DHCS and DHCS-S samples are shown in Figure 2 A. The

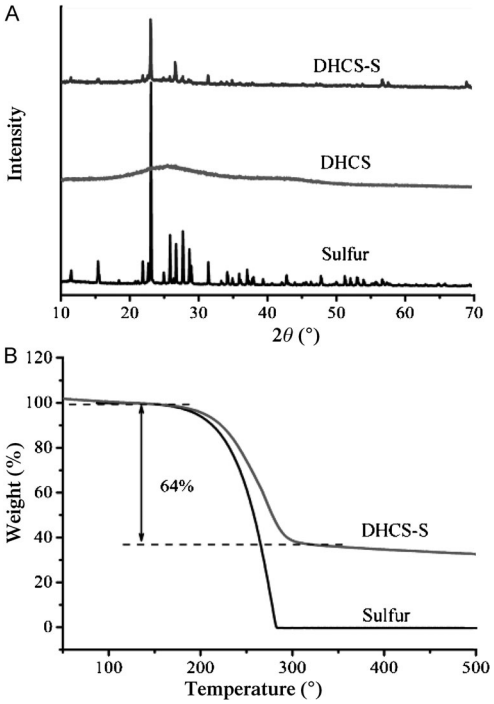

Figure 2. A) XRD patterns of sulfur, DHCS, and DHCS-S. B) TGA curves of sulfur and DHCS-S.

main diffraction peaks of graphitic carbon could hardly be recognized in the pattern of the DHCS sample, suggesting a generally amorphous nature for the carbon material. Meanwhile, the sulfur in the DHCS-S composite exists in a crystallized form. However, the broadened diffraction peaks with much reduced intensity compared with that of pure elemental sulfur indicate the small size of the sulfur crystallites (Table S1), which is in good agreement with the above FESEM and TEM images. Thermogravimetric analysis (TGA) of the DHCS-S composite in nitrogen flow showed a weight loss of approximately 64 % between 200 °C and 300 °C, which corresponds to the evaporation of sulfur in the composite materials (Figure 2 B). Hence the sulfur content in the DHCS-S sample was determined to be approximately 64 wt %. Moreover, compared with pure elemental sulfur, the sulfur component in the composite evaporates at a slightly elevated temperature. This is likely due to the strong interaction of carbon and sulfur, and the good encapsulation capability of the DHCSs.[10]

To demonstrate the possible structural advantages of the DHCSs, a carbon–sulfur nanocomposite using carbon black (CB) was also prepared for comparison. Following conven-

tional sulfur impregnation,[6] the sulfur content in the CB–sulfur composite (denoted as CB-S) was determined by TGA to be approximately 70 wt% (Figure S4). The evaporation temperature of sulfur in the CB-S composite, which was lower even than that of pure sulfur, indicated the weak interaction between carbon black and embedded sulfur. The typical cyclic voltammograms (CV) of the DHCS-S and CB-S composites are shown in Figure S5. Two pairs of current peaks are identified in the CV curve of the CB-S composite. The first pair of redox peaks at around 2.2 V and 2.8 V corresponds to the conversion between elemental sulfur (S_8) and soluble polysulfides, while the less pronounced pair at around 1.7 V and 2.4 V matches the conversion between polysulfide and insoluble Li_2S_2/Li_2S.[6,11] For the DHCS-S nanocomposite, current peaks in the CV curve were found in similar potentials compared to that of CB-S. However, the two pairs of current peaks were of comparable intensity, which suggests that the redox reactions, especially the conversion between polysulfide and Li_2S_2/Li_2S, were more facilitated in the DHCS-S composite during the CV scan.

The charge/discharge profiles within a cut-off voltage window of 1.5–3 V, as shown in Figure 3 A,B, were generally in agreement with the CV results. Two plateaus at around 2.3 and 2.0 V were observed in the discharge process, which are the typical characteristics of sulfur–carbon cathodes.[6,11] The CB-S composite showed a discharge capacity of 964 mA h g^{-1} (based on the mass of sulfur) in the first cycle, which droped to 760 mA h g^{-1} in the second cycle and kept decreasing afterwards (Figure 3 A). For the DHCS-S composite, a slightly higher discharge capacity of 1020 mA h g^{-1} was obtained during the initial discharging. More importantly, the capacity remained at 935 mA h g^{-1} in the second cycle and much better capacity retention was demonstrated (Figure 3 B). The good overlap of the discharge plateaus during the cycling test also suggested the good stability and reversibility of the electrode. Figure 3 C gives the cycling performance of the carbon–sulfur composites. At a constant current density of 0.1 C (167.5 mA g^{-1}), the DHCS-S composite showed much better cycling stability with a reversible capacity of 690 mA h g^{-1} after 100 cycles. In contrast, the discharge capacity of CB-S steadily dropped to 243 mA h g^{-1} by the 100th cycle, which was less than half of the value for DHCS-S. At a higher current rate of 0.3 C, the capacity of CB-S quickly dropped to about 100 mA h g^{-1} within 50 cycles, whereas the DHCS-S still delivered a discharge capacity of 410 mA h g^{-1} after 100 cycles (Figure S6). The superior capacity retention of the nanostructured DHCS-S composite can probably be attributed to the novel hollow structure of the carbon spheres, in which the highly porous network formed by the interconnected double shells serves as an excellent carbon host to encapsulate sulfur nanocrystallites. During the repeated charge/discharge of the electrode, the outward migration of dissolved polysulfides and the loss of active material were greatly suppressed by the complex double-layered shells as evidenced by the relatively high Coulombic efficiency (Figure S7). Meanwhile, the flexible character of the carbon host and the hollow structure could effectively mitigate the structural degradation caused by the volume expansion upon full lithiation.[17] The rate capability of the composite materials is shown in Figure 3 D. The discharge capacity gradually decreased as the current rate increased from 0.1 C to 1 C. A satisfactory capacity of 350 mA h g^{-1} was obtained for DHCS-S at 1 C (1675 mA g^{-1}), and the material recovered most of the capacity when the current rate was reduced back to 0.1 C. The rate performance of the DHCS-S composite was much better than that of the CB-S, likely because of the facile electronic/ionic transport and improved reaction kinetics in the DHCSs.

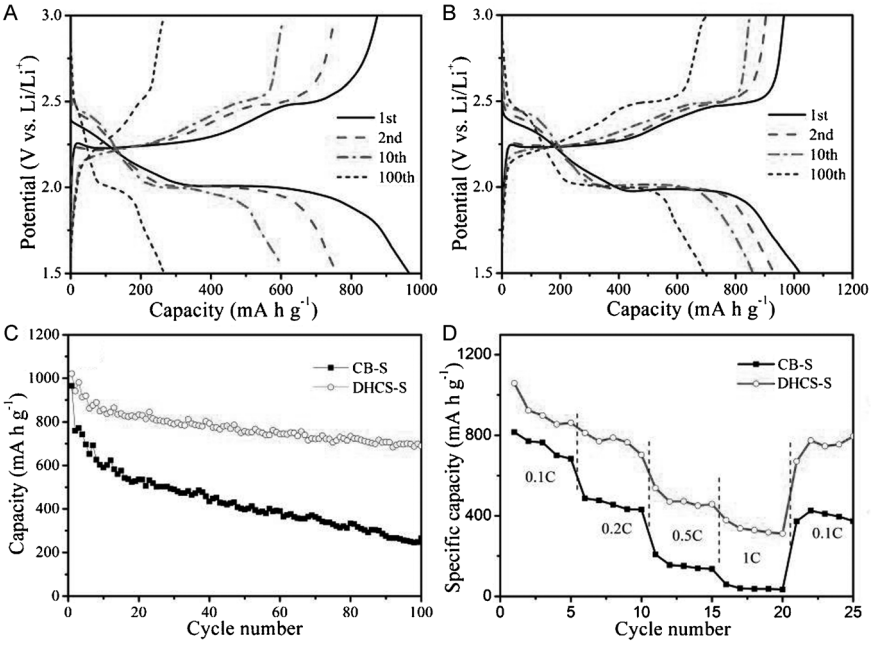

Figure 3. Discharge/charge voltage profiles of A) CB-S and B) DHCS-S electrodes at a current density of 0.1 C. C) Cycling performance of CB-S and DHCS-S at a current density of 0.1 C. D) Rate capabilities of the CB-S and DHCS-S.

In summary, we have successfully synthesized a new carbon–sulfur nanocomposite by effectively confining sulfur in double-shelled hollow carbon spheres. These unique concentric double shells are connected by carbon "links" to form a highly porous structure. Such complex hollow carbon spheres gave rise to a high surface area and pore volume to effectively encapsulate a substantial amount of sulfur, and suppressed the diffusion of dissolved polysulfides at the same time. In addition, the electronic/ionic transport and the ability to accommodate volume variation were also improved, owing to the unique hollow structure of the carbon host. As a result, when evaluated as a cathode material for lithium–sulfur batteries, the carbon–sulfur nanocomposite gave superior electrochemical performance with

high specific capacity, and excellent cycling stability and rate capability.

Received: July 5, 2012
Published online: August 17, 2012

Keywords: cathode · composites · electrochemistry · hollow structures · lithium–sulfur batteries

[1] B. L. Ellis, K. T. Lee, L. F. Nazar, *Chem. Mater.* **2010**, *22*, 691.
[2] X. Ji, L. F. Nazar, *J. Mater. Chem.* **2010**, *20*, 9821.
[3] P. G. Bruce, S. A. Freunberger, L. J. Hardwick, J.-M. Tarascon, *Nat. Mater.* **2012**, *11*, 19.
[4] S. E. Cheon, K. S. Ko, J. H. Cho, S. W. Kim, E. Y. Chin, H. T. Kim, *J. Electrochem. Soc.* **2003**, *150*, A796.
[5] J. Shim, K. A. Striebel, E. J. Cairns, *J. Electrochem. Soc.* **2002**, *149*, A1321.
[6] X. Ji, K. T. Lee, L. F. Nazar, *Nat. Mater.* **2009**, *8*, 500.
[7] J. A. Dean, *Lange's Handbook of Chemistry*, 15th ed., McGraw-Hill, **1998**.
[8] Y. V. Mikhaylik, J. R. Akridge, *J. Electrochem. Soc.* **2004**, *151*, A1969.
[9] S. E. Cheon, K. S. Ko, J. H. Cho, S. W. Kim, E. Y. Chin, H. T. Kim, *J. Electrochem. Soc.* **2003**, *150*, A800.
[10] C. Liang, N. J. Dudney, J. Y. Howe, *Chem. Mater.* **2009**, *21*, 4724.
[11] N. Jayaprakash, J. Shen, S. S. Moganty, A. Corona, L. A. Archer, *Angew. Chem.* **2011**, *123*, 6026; *Angew. Chem. Int. Ed.* **2011**, *50*, 5904.
[12] B. Zhang, X. Qin, G. R. Li, X. P. Gao, *Energy Environ. Sci.* **2010**, *3*, 1531.
[13] R. Elazari, G. Salitra, A. Garsuch, A. Panchenko, D. Aurbach, *Adv. Mater.* **2011**, *23*, 5641.
[14] J. Guo, Y. Xu, C. Wang, *Nano Lett.* **2011**, *11*, 4288.
[15] L. Ji, M. Rao, S. Aloni, L. Wang, E. J. Cairns, Y. Zhang, *Energy Environ. Sci.* **2011**, *4*, 5053.
[16] L. Ji, M. Rao, H. Zheng, L. Zhang, Y. Li, W. Duan, J. Guo, E. J. Cairns, Y. Zhang, *J. Am. Chem. Soc.* **2011**, *133*, 18522.
[17] G. Zheng, Y. Yang, J. J. Cha, S. S. Hong, Y. Cui, *Nano Lett.* **2011**, *11*, 4462.
[18] S. Evers, L. F. Nazar, *Chem. Commun.* **2012**, *48*, 1233.
[19] J. Schuster, G. He, B. Mandlmeier, T. Yim, K. T. Lee, T. Bein, L. F. Nazar, *Angew. Chem.* **2012**, DOI: 10.1002/ange.201107817; *Angew. Chem. Int. Ed.* **2012**, DOI: 10.1002/anie.201107817.
[20] Z. Dong, X. Lai, J. E. Halpert, N. Yang, L. Yi, J. Zhai, D. Wang, Z. Tang, L. Jiang, *Adv. Mater.* **2012**, *24*, 1046.
[21] X. Lai, J. E. Halpert, D. Wang, *Energy Environ. Sci.* **2012**, *5*, 5604.
[22] X. Lai, J. Li, B. A. Korgel, Z. Dong, Z. Li, F. Su, J. Du, D. Wang, *Angew. Chem.* **2011**, *123*, 2790; *Angew. Chem. Int. Ed.* **2011**, *50*, 2738.
[23] X. W. Lou, Y. Wang, C. L. Yuan, J. Y. Lee, L. A. Archer, *Adv. Mater.* **2006**, *18*, 2325.
[24] X. W. Lou, D. Deng, J. Y. Lee, L. A. Archer, *Chem. Mater.* **2008**, *20*, 6562.
[25] J. S. Chen, C. M. Li, W. W. Zhou, Q. Y. Yan, L. A. Archer, X. W. Lou, *Nanoscale* **2009**, *1*, 280.
[26] X. W. Lou, J. S. Chen, P. Chen, L. A. Archer, *Chem. Mater.* **2009**, *21*, 2868.

